RSC Advances

ROYAL SOCIETY OF CHEMISTRY

www.rsc.org/advances

Novel fluorescent security marker. Part II: Application of novel 6-alkoxy-2-amino-3,5-pyridinedicarbonitriles nanoparticles in safety paper.

Altaf Basta,[1*] Mauro Missori[2*], Adel S. Girgis,[3] Marco De Spirito,[4] Massimiliano Papi.[5] and. Houssni El-Saied.[1]

1) Cellulose and Paper Dept., National Research Centre, Dokki-12622, Cairo, Egypt

2) Istituto dei Sistemi Complessi, Consiglio Nazionale delle Ricerche, Via Salaria Km 29.300, 00016 Monterotondo Scalo (Rome), Italy

3) Chem. Pesticide Dept., National Research Centre, Dokki-12622, Cairo, Egypt

4) Istituto di Fisica, Università Cattolica del Sacro Cuore, Largo F. Vito 1, 00168, Rome,Italy

5) Facoltà di Medicina e Chirurgia, Università Cattolica del Sacro Cuore, Largo F. Vito 1, 00168, Rome,

ABSTRACT

Application of newly fluorescent nanoparticles of 6-alkoxy-2-amino-3,5-pyridinedicarbonitriles as security marker for enhancing the safety property of bagasse-based paper sheets (as valuable documents) was studied. The role of sonication conditions and type of molecule (morpholynile or piprydinyl) containing heterocyclic compound on production of nanoparticles and their fluoresce behaviour were evaluated. The quality of the obtained treated paper was evaluated from examining the fluorescence behavior of the particles treated paper sheets, in comparison with their fluorescence behavior in water suspension. Success of these investigated fluorescent particles as security marker was recommended from examining the strength properties of the treated paper and the interaction between the fluorescence particles and cellulose fibers, via FTIR-spectra and thermal stability tests, moreover, from the unfalsifiable safety of the treated documents by erasures technique (Chemical and mechanical).

Key-words: *3,5-pyridinedicarbonitrile,* Fluorescent particles, Reprecipitation method, Organic fluorescent particles, Pyridine derivatives, Security marks, Unfalsifiable documents, Safety paper

*To whom correspondence should be addressed. A. H. Basta. Tel:+201222174239 . Fax: +202-33371719 . E-mail: altaf_basta@yahoo.com. M. Missori. Tel: +39-06-49934166. Fax: +39-06-49934168. E-mail: mauro.missori@isc.cnr.it

1. Introduction

Paper represents a major product of lignocellulosic materials (agro- and wood). Special papers are used for specific purposes such as; water proof paper, carbon paper, cast-coated paper, durable documents, decorative papers, electrical and magnetic paper, etc. Many literature concerned on the role of cellulosic fibers, sizing agent, metal complexes, fire retardant additives, coated biopolymers, surrounding environment on the quality and durability of paper [1-9]. Safety or functional papers are very special grade of paper having a surface design or hidden warning indicia or both of such marks as to make obvious any attempt of fraudulent alteration of writing there on by ink eradicators, mechanical erasure…etc. Such paper is used for bank check, tickets, postal money orders or other papers having a negotiable value [10].

The majority of safety papers currently available on the market reactivate quietly to such attempts of falsification with ink-erasing pencils. This often causes the appearance of a fluorescent yellow color which is not easily visible to the naked eye and which furthermore prove troublesome for certain uses [11]. Several methods and systems to mark and protect from falsification valuable documents made of, or supported on paper, are based on the use of secret fluorescent dyes [12]. In this context, 2-alkoxy-3-pyridinecarbonitrile derivatives have been synthesized [12, 13]. These derivatives exhibit remarkable fluorescence properties enabling their employment on paper sheets prepared from non-wood fibrous material (bagasse pulp) to produce security paper. However, while these secret dyes show intense fluorescence and leave unaffected the paper substrate on which they are deposited, known problems include low resistance to chemical degradation and photodegradation [12]. In addition, optical properties are specific of each compound and cannot be modified. The same authors [14], succeeded in synthesized of a variety of pyridine derivatives possessing both the aforementioned functional groups i.e. amino and alkoxy groups oriented *o*- and *o*'-positions of the pyridine nucleus and neighboring to nitrile functions. In other words, gathering the whole functional moieties responsible for fluorescence properties in a sole structure system in an attempt to optimize a fluorescence active agent with high quantum yield.

On the other hand, fluorescent nanoparticles of organic molecules are attracting increasing interest for their good fluorescence quantum yield and long stability over time [15- 19]. The electronic and the optical properties of organic nanoparticles, due to weaker intermolecular forces such as hydrogen bonds, van der Waals and hydrophilic/hydrophobic interactions, can easily be modulated to obtain many unusual optical properties and potentially useful emission [20, 21].

In particular, when the relative orientation of the transition dipole moments of molecules in nanoparticles results in a head-to-tail arrangement, a so-called J-aggregate is formed [20]. The

optical properties of this structural packing are characterized by the shift of the excitonic band towards lower energy with respect to the absorption of the monomers (bathochromic shift), and high fluorescence quantum yield [22]. The opposite behaviour is found for parallel arrangement of dipole moments (H-aggregates), with excitonic absorption at higher energy than that of the isolated molecule (hypsochromic shift) and quenching of fluorescence [21].

When the organic nanoparticles tend to be unstable in solution, often aggregating or precipitating over the course of few days [22], their use is therefore severely hampered. Therefore advances have been gained by adopting the reprecipitation method. This method consists in injecting a dilute solution of monomers into a poor solvent. Being insoluble, monomers aggregate and form a colloidal suspension of particles**,** which size ranges from nanometers to micrometers [23, 24]. To control particles size, sonication was used during the reprecipitation process [25-27]. Sonochemical preparation of nanophase materials relies on acoustic cavitation, which is the formation, the growth and implosive collapse of bubbles in a liquid irradiated with high-intensity ultrasound [28]. The extremely high temperatures (~ 4000 K in water), pressures (>20 MPa) and cooling rates (>10^7 K s^{-1}) attained during acoustic cavitation inside of the collapsing bubbles are exploited to initiate chemical reactions such as oxidation, reduction, decomposition and promotion of polymerization [29, 30]. Although details on the formation of organic nanoparticles under sonication still need further investigation, acoustic cavitations seems to be the most probable driving force providing the energy needed in the formation of small nuclei [25].

Converting the previous investigated 2-Amino-6-ethoxy-4-[4-(4-morpholinyl)phenyl]-3,5-pyridinedicarbonitrile (AEMP), fluorescence active prepared heterocycles to nanoparticles of sizes range from tens to hundreds of nanometers, was provided by the combination of reprecipitation and sonication [27]. This method provides an effective way to produce fluorescent organic nanoparticles for several applications that rely on strong and stable fluorescence, as possible for marking important or valuable documents. The surprising results were that the suspension of nanoparticles was found to be stable for more than two years when stored at 4 °C in darkness. It was also found that, a remarkable increase in the fluorescence yield was observed as nanoparticles sizes decrease. The above features, together with the striking stability of optical and mechanical properties over the course of months, allow for straightforward applications that rely on strong and stable fluorescence such as marking important documents.

These results persuaded us for surface application of AEMP on valuable documents (unfalsifiable safety paper). To the best of our knowledge, this work is the first work about fluorescent organic nanoparticles that can be used as secret markers for paper documents. In parallel

experiments, *2-Amino-6-ethoxy-4-[4-(1-piperidinyl)phenyl]-3,5-pyridinedicarbonitril* particles (AEPP) was synthesized and surface treated the paper sheets.

The overarching objective of this present work is to assess the possibility of applying newly fluorescent nano-particles of 6-alkoxy-2-amino-3,5-pyridinedicarbonitriles, as security marker, for enhancing the safety property of bagasse-based paper sheets (as valuable documents). The role of sonication conditions and type of molecule (morpholynile or piprydinyl) containing heterocyclic compound on production nano-particles fluoresce compounds, and which fluorescence particles is more efficient for document quality, especially against strength and falsification were also optimized.

2. Experimental

2.1. Synthesis and characterization of fluorescent heterocyclic particles.

Synthesis of novel 6-alkoxy-2-amino-3,5-pyridinedicarbonitriles were prepared according to the previously reported procedures,[14] and was summarized with their analyses in the following methods and scheme (Scheme. 1).

***2-Amino-6-ethoxy-4-[4-(4-morpholinyl)phenyl]-3,5-pyridinedicarbonitrile* (AEMP or 3c).**

Reaction time 24h, almost colourless crystals from *n*-butanol, mp 234-236 °C, yield 40%. IR: $\nu_{max.}$/cm^{-1} 3492, 3371 (NH_2), 2223, 2211 (C≡N), 1617, 1574 (C=N, C=C). ^{1}H-NMR ($CDCl_3$): δ 1.35 (t, 3H, CH_3, J = 7.2 Hz), 3.21 (t, 4H, morpholinyl 2 NCH_2, J = 4.8 Hz), 3.80 (t, 4H, morpholinyl 2 OCH_2, J = 4.8 Hz), 4.38 (q, 2H, O*CH*$_2$CH$_3$, J = 7.2 Hz), 5.48 (s, 2H, NH_2), 6.94 (d, 2H, arom. H, J = 8.7 Hz), 7.43 (d, 2H, arom. H, J = 8.7 Hz). MS: *m/z* (%) 349 (100). Anal. for $C_{19}H_{19}N_5O_2$ (349.38): Calcd., C 65.31, H 5.48, N 20.05; Found: C 65.27, H 5.38, N 20.23%.

***2-Amino-6-ethoxy-4-[4-(1-piperidinyl)phenyl]-3,5-pyridinedicarbonitrile* (AEPP or 3d).**

Reaction time 24h, pale yellow crystals from *n*-butanol, mp 246-248 °C, yield 46%. IR: $\nu_{max.}$/cm^{-1} 3431, 3343, 3234 (NH_2), 2212 (C≡N), 1640, 1605 (C=N, C=C). ^{1}H-NMR ($CDCl_3$): δ 1.34 (t, 3H, CH_3, J = 7.2 Hz), 1.50-1.64 (m, 6H, piperidinyl 3 CH_2), 3.24 (t, 4H, piperidinyl 2 NCH_2, J = 5.7 Hz), 4.37 (q, 2H, O*CH*$_2$CH$_3$, J = 7.2 Hz), 5.46 (s, 2H, NH_2), 6.93 (d, 2H, arom. H, J = 8.1 Hz), 7.40 (d, 2H, arom. H, J = 9.0 Hz). MS: *m/z* (%) 347 (100). Anal. for $C_{20}H_{21}N_5O$ (347.41): Calcd., C 69.14, H 6.09, N 20.16; Found: C 68.91, H 5.90, N 20.38%.

According to the data of fluorescence behavior (quantum yield), the synthesized *2-Amino-6-ethoxy-4-[4-(4-morpholinyl)phenyl]-3,5-pyridinedicarbonitrile* (**3c**), possess higher quantum yield (ϕ_s relative to the fluorescence quantum yield of quinine sulfate, is reached ~0.83 [14]).

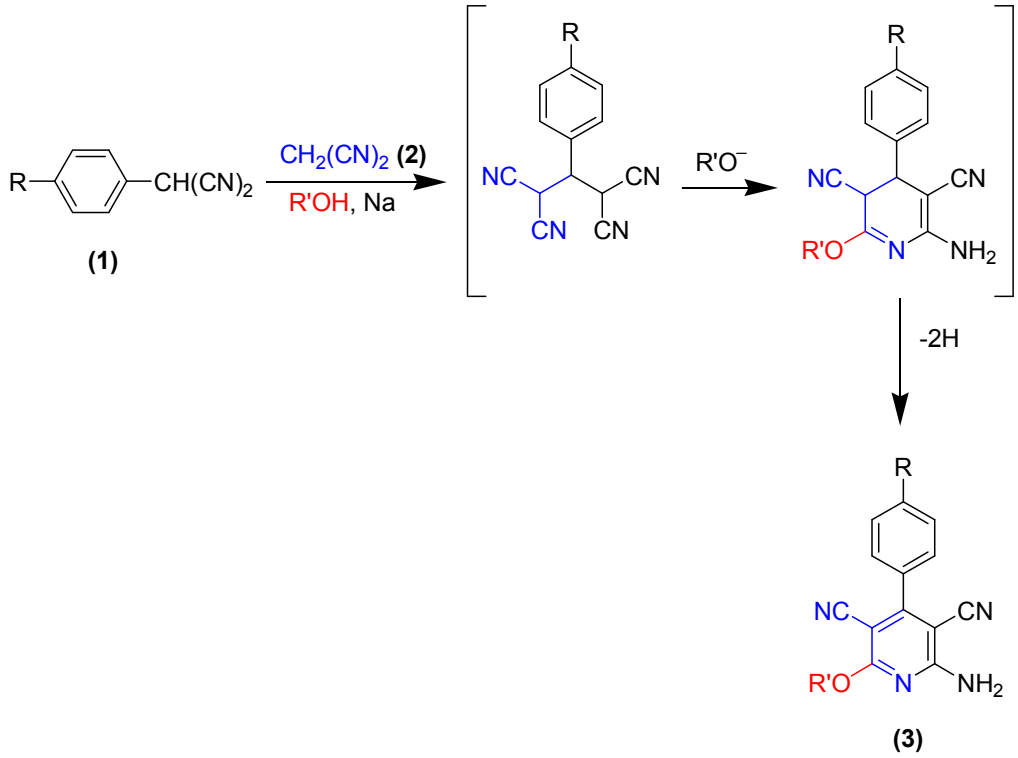

1a, R = 1-piperidinyl

1b, R = 4-morpholinyl

3c, R = 4-morpholinyl, R' = C_2H_5

3d, R = 1-piperidinyl, R' = C_2H_5

Scheme (1)

2.1.1. Production of the AEMP and AEPP particles

Nano- and microparticles of fluorescent 3c (AEMP) and 3d (AEPP) heterocyclic compounds were obtained by the reprecipitation method under sonication. Particles were prepared with 100 µL of acetone solutions of AEMP and AEPP (1 mM), injected into 10 mL of de-ionized and 0.2 µm filtered water used as a non-solvent environment [23, 31] (see Table 1 for more details).

Sonication was induced by a Vibra-Cell ultrasonic processor (Sonics & Materials, Inc., USA), at power 12.5 W (see Table 1), connected to a titanium horn to radiate the ultrasonic energy to the liquid contained in a beaker. The beaker was kept in a thermostatic bath to maintain the water at

0°C of temperature during the sonication process. The sonication conditions were selected based on the previous study [27], in order to obtain smaller nanoparticles avoiding their degradation. Therefore we used smaller power and low solution temperature and sonication time for 3c and 3d compound.

2.1.2. Dynamic Light Scattering

The size of the resulted sonicated fluorescent heterocyclic particles has been assessed by using Dynamic Light Scattering (DLS) [32]. DLS is a well established, nondestructive technique, allowing the sizing of particles in solution with high accuracy [33]. Here measurements were carried out with a commercial light-scattering setup Zetasizer Nano ZS (Malvern), that use a Non-Invasive Backscatter (NIBS) optics, with the scattering angle fixed at 173º. This specific setup allows detecting the autocorrelation function of diffusing particles with size ranging from 0.3 nm to 10 μm. DLS data were analyzed by using the regularized Laplace inversion of the intensity autocorrelation function (CONTIN method) [34], CONTIN method has been used to obtain the intensity-weighted hydrodynamic radii distribution of particles [35]. The hydrodynamic radius, defined as $R_h = \frac{kT}{4\pi D\eta}$, where k is the Boltzmann constant, T is the absolute temperature, D is the diffusion coefficient and η is the water viscosity, represents the radius of a hypothetical hard sphere that diffuses in water with the same speed of the particle under examination [36].

2.1.3. Optical Properties.

Optical absorption of fluorescence compounds solutions and their particles dispersed in water were measured in the 200–880 nm wavelength (λ) range by using an Ocean Optics fiber spectrophotometer (model USB 2000). The detector is a 2048 pixels linear silicon CCD. The optical setup allows a spectral resolution of 1 nm FWHM; while data were pitched every 0.38 nm. Quartz cuvette with 1 cm optical path length was used to house water suspension of particles. All absorption measurements were normalized to water filled quartz cuvette.

Excitation spectra and photoluminescence emission of AEMP and AEPP heterocyclic fluorescent particles dispersed in water and on paper substrate were carried out by using a Perkin-Elmer LS 45 fluorescence spectrometer. Quartz cuvette with 1 cm optical path length was used to house the samples. The spectral resolution was 10 nm and data were pitched every 0.5 nm.

Front-surface excitation and collection geometries were used for the investigation of photoluminescence spectra of particles on paper substrate.

2.2. Paper sheets treated and tests

The paper sheets composition is 80% of bleached kraft bagasse pulp and 20% of bleached kraft softwood pulp. Kaolin (around 10%) and alum–rosin are used as filler and sizing materials, respectively. This paper sheets were kindly delivered from Quena Co. for paper production- Upper Egypt. The bagasse-based paper sheet were sprayed by the fluorescence particles compounds (3c,3d**)**, suspended in deionized water, using automatic atomizer to achieve high degree of homogeneity distribution over one phase of sheet (1.4- 1.82 g /m^2 , SD ± 0.03-0.608). The samples were dried, and then conditioned at 20^{o}C and 50% RH [37].

Strength properties, e.g., tensile, tear, and burst indices of paper samples were measured before and after treatment, according to Standard procedure [38]. Surface ultra-violet examination was carried out by using Documenter$^{(R)}$ 4500, Spectral Analysis System (Projectina, Swiss).

2.2.1. Interaction between fluorescence heterocyclic particles and paper surface

To investigate interactions between paper and sonicated-florescent compounds, IR-spectra were carried out by using a FT/IR-6100 Jasco, Japan (using Attenuated Total Reflection; ATR), on samples of paper. A resolution of 4 cm^{-1} was used in the measurements. The mean strength of hydrogen bond (MHBS) was calculated according to Levidic et al [39].

The paper samples were subjected to non-isothermal thermogravimetric analysis. Thermogravimetric analyses were performed in a Perkin Elmer Thermogravimetric Analyzer TGA7. The samples were heated in pure nitrogen (flow rate 50 mL/min) at 10 °C /minute, and within the typical temperature range: 35 – 600 ^{o}C, i.e., till no additional weight loss was observed. Measurements were made using calcined alumina as reference material. Differential thermogravimetric (DTG) peaks were examined for evidencing different behaviours between the samples, and also for understanding how the surface treatments affected the thermal stability of fibers. The kinetic parameters based on the weight loss data of TG curve analysis were determined according to the equations described elsewhere [40, 41].

TG-curve analysis

Kinetic studies, based on the weight loss data, were obtained by TG curve analysis. The activation energy has been evaluated according to Coat and Redfern method [40]. For pseudo

homogeneous kinetics, the irreversible rate of conversion of the weight fraction of reactant was expressed by the following equation:

$$\frac{d\alpha}{dt} = k\,(1-\alpha)^n \qquad (1)$$

where, α is the fraction of material decomposed at time t, k is the specific rate constant and n is the order of reaction. The temperature dependence of k is expressed by the Arrhenius equation:

$$k = A\,e^{Ea/RT} \qquad (2)$$

where, A is the frequency factor (s^{-1}) and T is the absolute temperature.

For linear heating rate, a, (deg.$min.^{-1}$):

$$\alpha = \frac{dT}{dt} \qquad (3)$$

The activation energy, Ea, of thermal decomposition when n = 1, was calculated by using equation 4.

$$\log\left[-\log\frac{1-\alpha}{T^2}\right] = \log\frac{AR}{\alpha E_y}\left[1-\frac{2RT}{E_a}\right] - \frac{E_a}{2.3\,RT} \qquad (4)$$

When n ≠ 1, equation 5 was used;

$$\log\left[\frac{1-(1-\alpha)^{1-n}}{T^2(1-n)}\right] = \log\frac{AR}{\alpha E_a}\left[1-\frac{2RT}{E_a}\right] - \frac{E_a}{2.3\,RT}$$

Plotting the left-hand-side value of the equation { i.e., log [1- $(1-\alpha)^{1-n}$ / T^2 (1-n)]} against 1 / T using various values of "n" should give a straight line with the most appropriate value of "n". [41] The Least square method was applied for the equation, using values of "n" ranging from 0.0 to 3.0 in increments of 0.5 [41]. The correlation coefficient (r) and the standard error (SE) were calculated for each value of "n". The "n" value, which corresponds to the maximum r and minimum SE, is the order of the degradation process. The activation energies and frequency factors were calculated

from the slope and intercept, respectively, of the Coat-Redfern equation with the most appropriate value of "n".

2.2. Unfalsifiable safety examination

For unfalsifiable safety examination, chemical and erasures were used to study the effectiveness of erasures on the fluorescence behavior of paper sheets that were sprayed with particles of AEMP and AEPP fluorescent compounds subjected to different sonication processes.

In all eradicators, the Ballpoint ink (Rynolds)® type, the erasing of ink by chemical agents (e.g., eradicators; commercial alkaline Clorox® (NaOCl), or benzylalcohol), from different examined hand sheet papers done using a piece of cotton moistened with the erasure solution, and the wiping was done several times carefully with ethanol to avoid destruction of paper or removal of fiber from the surface of the paper as possible. While, the eradication via mechanical was done using eraser Papers were examined visually with naked eye and by ultraviolet device by Docucenter(R) 4500 instrument at wavelength 365 nm.

3. Results and Discussion

3.1. Dynamic Light Scattering and optical properties of sonicated novel 6-alkoxy-2-amino-3,5-pyridinedicarbonitriles particle

The use of controlled sonication conditions during the reprecipitation in water has been demonstrated to be a valid method to control both the size and crystallinity of organic nanoparticles.[22, 25, 26] The sonication parameters were chosen to avoid AEMP and AEPP compounds degradation during the preparation process. The sonication power was kept constant at 12.5 W. Sonication processes result in a mass loss as compared to the mass of the AEMP or AEPP molecules injected into the water. For 12.5 W sonication power, a final mass concentration of particles around 2–3% of the injected value is expected [27]. The yield of the particles production process at 12.5 W sonication power could be explained as due to the interplay between the efficiency in the formation of nanoparticles nuclei and AEMP or AEPP molecules degradation. In addition, water dissociation induced by ultrasonic energy and the formation of short lived radical species, could play an important role in the nanoparticles formation process [42].

The mean hydrodynamic radii, $\langle R_h \rangle$ together with the polydispersity index of the size distribution ($\sigma/\langle R_h \rangle$) and the zeta potential are reported in Table 1. Zeta potential is the electric potential between nanoparticles which is correlated to the stability of the nanoparticles suspension.

The mean hydrodynamic radii $\langle R_h \rangle$ and the polydispersity index of the AEMP and AEPP particles dispersed in water are shown in Figure 1.

DLS measurements showed that the sonication process time has a profound effect beside the included groups of novel *6-alkoxy-2-amino-3,5-pyridinedicarbonitriles*. AEMP and AEPP samples show two distinct behaviors of $\langle R_h \rangle$ and $\sigma/\langle R_h \rangle$ with sonication time. For sample containing morpholynile group (AEMP; 3c), a maximum value of $\langle R_h \rangle$=479 nm was observed for 1 minute of sonication time. A smaller particle size was obtained with 5 minutes of sonication time while extending the sonication time to 30 min resulted in the smallest size of 97 nm. The polydispersity index, instead, decreased from 0.79 to 0.33 and rise slightly to 0.40 with increasing the time from 1, to 5 and finally to 30 min (Table 1 and Figure 1).

As can be noted that all the average sizes of piperidinyl- containing fluorescence compounds (AEPP; **3d**) are lie in hundred nanometres. Particle sizes are less affected by the sonication time, especially when extending the time from 5 min to 30 min, where the particle sizes were 224 nm, and 240 nm and polydispersity index were about 0.49 and 0.58, respectively. It could be concluded that substituting the morpholynile groups by piperidenyl groups in the investigated fluorescence heterocyclic compounds does not provide particles in nano-scale, but all in hundreds of nanometer scale.

The zeta potential, which indicates the electrical potential between nanoparticles, of the AEPP is two times of AEMP, indicating the stability of sonicated particles of AEPP fluorescent compound than AEMP.

UV-Vis absorption spectra of AEMP and AEPP sonicated particles, in water suspension, are shown in Figure 2. For AEMP particles in water suspension two maxima in the absorption spectra (Figure 2) at about 340 nm (3.65 eV) and 370 nm (3.35 eV), and a tail toward longer wavelength, are evident, in agreement with previously published results [27]. The spectroscopic features have been assigned to the n–π* and π–π* transitions of pyridine nuclei of AEMP molecules in nanoparticles, and a charge-transfer (CT) exciting band of the extended crystal structure, as previously observed in the absorption spectra of other organic nanoparticles [15, 22]. For AEPP particles in water suspension only one shoulder at about 325 nm in the absorption spectra is evident (Figure 2-a).

The fluorescence excitation spectra of AEMP and AEPP nanoparticles with 5 minutes of sonication time, displayed in the lower panel of Figures 2-b and 2-c, show similar features to those of the absorption spectra in Figure 2-a.

It is obvious that the synthesized morpholine containing heterocyclic compounds (AEMP**)** exhibits two excitation bands peaked at a wavelength of about 340 nm, and 375 nm; while piperidinyl containing compound (AEPP) have only one excitation band peaked at a wavelength of about 335 nm, corresponding to UV absorption maxima (Figure 2-a). However, one intense emission band was observed for both compounds at a wavelength of 400-540 nm when exciting at 360 nm. The emission band in the morpholinyl containing compounds is broader with maximum at higher wavelength (458 nm), and shoulder at 550 nm, than piperidinyl containing compound (only at 432.5nm). The best fluorescence is obtained when the morpholine (AEMP**)** ring was introduced comparable with piperidinyl ring (AEPP).

3.2. Evaluation of surface treated paper sheets

Due to the possible application of the investigated novel fluorescence compounds as security marks of value documents, the fluorescence character at moderate sonication time, 5min, was investigated on paper substrate. We have measured the emission spectra and intensity of the emission band in surface treated local bagasse paper sheets, using an excitation wavelength of 360 nm. In this respect, the specific amounts of water suspension of nanoparticles have been centrifuged and the supernatant solution has been removed to increase the nanoparticles concentration by a factor of 10. The concentrated water suspensions of nanoparticles were sprayed on local bagasse-base paper sheets described in Paragraph 2.2. Their fluorescence properties are illustrated in Figures 2-b and 2-c, in comparison with the fluorescence of sonicated particles suspended in water.

Figures 2-b and 2-c show that the position of emission bands of paper treated with morpholinyl-containing fluorescent compounds (**S2,** AEMP) were shifted to shorter wavelength (red shift 18.5 nm) compared to that treated with piperidinyl-containing compound (**S5**, AEMP); (blue shift 7 nm); both with respect to the emission of fluorescent samples in water. This is ascribed to probable interaction of functional groups containing fluorescent compound with hydroxyl and carbonyl groups containing paper sheets. This may affects on functional moieties responsible for fluorescence properties (6-alkoxy-2-amino-4-aryl-pyridine functional groups). The presence of lone-pair electron of oxygen in morpholinyl ring may promote this interaction effect. This view is in agreement with the assumption reported before that, the strong interaction between AEMP and cellulose occurred due to a resonant energy transfer from cellulose to nanoparticles [12].

As can be seen, changing the substituted groups is accompanied by changing the position of emission band. The intensity of emission band, were nearly the same for paper sheet treated with the two sonicated compounds, **S2** and **S5**, despite weight gain on the paper are 1.3 g/m^2, and 1.7

g/m^2, respectively. The relatively lower weight gain of paper to morpholinyl containing compound not affected on both position and intensity of emission band, compared with relatively higher weight gain of piperidinyl compound (AEPP).

For the mechanical properties, the histograms of Figure 3 shows that treating the paper sheets made from bagasse with the investigated fluorescent compounds, in addition to provide the paper samples fluorescence character, it also improves the quality number, Q_z.. Quality number (Q_z) refers to the trend of all strength properties, e.g., breaking length, burst and tear factors, and number of double folds [41]. This observation is reverse to that observed in case of bagasse pulp-containing paper sheets treated with these unsonicated fluorescent compounds [14]. In other words, subjected the investigated fluorescent compounds to sonication reduced the bad effect of surface treated the local-bagasse paper surface with fluorescence compound. The extent of improving is not only dependent of fluorescent compound but depending also on average particle size. As can be seen, there is a good relation between the decreases of particle size, under the effect of sonication, with the improvement in quality number (Q_z). Moreover, treating with morpholinyl group.-containing fluorescence compound (AEMP; **3c**) achieves relatively high improvement in double fold property of paper sheets, compared with AEPP (**3d**). These data confirmed the presence of morpholinyl group instead of piperidinyl groups may enhances the interaction of fluorescence compounds with paper fibers and weaken the fiber-fiber hydrogen bonding.

It is interest to note that all treated paper sheets are characterized by relatively high strength properties (Q_z), compared to untreated local bagasse-based paper sheets.

3.3. Evidence of interaction of sonicated fluorescence compounds with paper samples.

The data of FT-IR measurements (Figure 4 and Table 2), emphasized the view of interaction of functional groups (NH_2) of fluorescence macro-and nano-particles with functional groups containing surface paper sheets, via hydrogen bonds. Whereas, the mean hydrogen bond strength (MHBS) in the most treated samples (0.934-1.225), is relatively higher than untreated paper sample (0.917). The presence of oxygen in hetero-ring, e.g., morpholinyl or sonication at relatively lower period restricted the formation of hydrogen bonds, whereas the MHBS of paper treated with AEMP and sonicated for 1 min is 0.862. This negative action is minimized at relatively lower particle size. Also the band corresponds to OH symmetric and asymmetric stretching vibration of untreated paper sample is higher red shift on treated with **S2** (shifted from 3332 cm^{-1} to 3281 cm^{-1}); while there's no shift in band position on treating with **S5**. The bands correspond to bending vibration of OH and NH, at ~ 1450 cm^{-1} behaves the same trend. The appearance of more than one band correspond to

C-O-C and/or C-N-C in cyclic compounds in FT-IR spectra of samples **S1**-**S6** confirmed the inclusion of morpholinyl- or piperidinyl containing compounds (AEMP, AEPP) on paper samples. For the case of surface treatment with piperidinyl containing compounds (S4-S6), the increase in the bands at ~ 2920, ~ 2860 cm^{-1}, or split the band correspond to (C=C or and C=N), at 1640-1655 cm^{-1}, is noticed, especially for sample **S6**; sonicated at 30 min, with smaller particle size (240 ±139 nm), and higher weight gain. (1.83 g/m^2).

For all surface treated paper samples by AEPP, the relative absorbance's of bands related to C=O or C=N decreased, and the bands corresponds to OH is shifted to lower wave-length with increasing the MHBS. The foregoing results concluded that subjecting the fluorescence compounds, especially that containing morpholinyl compound, to sonication process; leads to motivate their application as security marker for high strength quality paper sheets.

Analysis of TGA curve also can be helpful in studying the thermal stability property which provides to local bagasse-based sheets by surface treatment with the investigated fluorescence compounds; especially with morpholinyl containing compounds (Table 3 and Figures. 5-a and 5-b). The TGA curves exhibit similar decomposition stages to the untreated paper samples, with the difference that only in onset temperatures and maximum peak temperature. Thermogravimetric (TGA and DTGA) degradation curves for untreated paper sheets are represented by Figure **5-a**, and three stages can be observed. The first stage, from 50- 102^oC represents the evolution of residually absorbed water that corresponds to 5.5% of the total weight. The second starts at 209.2 ^oC and ends at 343.1^oC, with peak maximum at 289.49^oC and occurs due to the depolymerization of paper components (cellulose & hemicellulose). This stage represents a prominent thermal degradation of weight loss of the cellulose to levoglucosan, with wt loss ~ 76.5%, and known as volatilization stage. The third stage occurs in the region of 380.6 – 470 ^oC and has a peak maximum at 438.8^oC, and occurs due to rapid volatilization accompanied by the formation of carbonaceous residue, with weight loss 96.8% (Table 3). For surface treated paper samples, the onset temperatures are (210-241^oC), and peak temperatures (296-307^oC). Also, their activation energies (Ea) for the main depolymerization stages are increased to 148-162 kJ/mole; while Ea for untreated paper is 131 kJ/mole. It is surprising to notice that, the surface treated with these investigated compounds retard the degradation, and leads to decrease the weight loss observed in the volatilization stage to about 75 %-70.5%, and the final degradation stages to about 95.2 - 90 %. This means that the fluorescent heterocyclic compounds in addition to provide thermal stability to paper sheets also exhibits to some extent fire resistance property to the produced treated paper. This view based on the main theory of flame retardance is to minimize the formation of levoglucosan by lowering the

decomposition temperature of cellulose and enhancing char formation by catalyzing the dehydration and decomposition reactions [43-45].

3.4. Chemical and mechanical erasures

Chemical and mechanical erasures were used to study their effectiveness on safety of surface treated bagasse-based paper sheets with the two candidate sonicated fluorescence heterocyclic compounds. Ballpoint ink (Rynolds®) was used for writing on the different treated hand-sheet paper. In this study, two types of chemical agents were used as eradicators; e.g., commercial alkaline Chlorox® (NaOCl), and benzyl alcohol in addition to mechanical erasure. For erasing to be made effective as much as possible, the area of the erasure was washed by ethanol (>85%) to extract any residual colored ink material.

From Figures 6-a and 6-b, it was noticed that sodium hypochlorite erasure had a great effect on erasing ink from both morpholinyl containing fluorescence compound (AEMP) and piperidinyl containing fluorescence compound (AEPP) treated paper sheets. This agent acts as a reducing agent for the ink colour and the erased area appears as a dark stain by ultraviolet light as it destroy the fluorescence behavior of the fluorescent compounds in this area.

For the case of benzyl alcohol followed by ethanol, when applied on ballpoint ink strokes that was written on treated paper sheets, it had a difficult effect on erasing ink color completely. So the erased area appears by ultraviolet light.

On comparing with untreated paper sheets, it was noticed that sodium hypochlorite or benzyl alcohol when applied for erasing ink color can not be detected easily and gave good erased sites without change the color of untreated paper itself. Time and trials require for erasing the ink colour from the paper increased in the case of paper treated with AEMP than AEPP. This view emphasized the highest surface bonding capacity of sonicated AEMP with relatively lower particle size (**S3**, $\langle R_h \rangle$= 97 nm). As can be noticed that eradicator by benzyl chloride was less effective for removing the ink stroke letter from treated paper produced from different sonicated fluorescent particles, and leaved zone appeared ultraviolet light. For AEPP-treated paper sheets this zone is appeared only for fluorescent particles resulted from sonication for 5and 30 min.

For mechanical erasure (Figures 6-a and 6-b), it was noticed that trails required for erasing the ink stroke from the treated paper sheets increased when the treated fluorescence particles resulted under sonication time 5 min and 30 min. Moreover, the mechanical erasure was less effective for removing the written letter than Benzyl chloride.

It was found that the shaved area was appeared as more intense fluorescence than neighboring non shaved area. So we can conclude that fluorescent compounds, especially with lower particle size, are penetrated inside paper sheets to a depth more than ink stroke itself.

4. Conclusion

Fluorescent heterocyclic compounds were applied to provide safety behavior of treated paper sheets. When, the nanoparticles promise significant improvement to their field of application, therefore in this study we subjected the synthesized 2-Amino-6-ethoxy-4-[4-(4-morpholinyl)phenyl]-3,5-pyridinedicarbonitrile (AEMP) and 2-Amino-6-ethoxy-4-[4-(4-pipredinyl)phenyl]-3,5-pyridinedicarbonitrile (AEPP) for sonication, as a trial to convert these fluorescent compounds to particles (AEMP and AEPP, respectively). Further application, as security marker, for enhancing the safety property of bagasse paper sheets (valuable documents) was assessed.

The application of the resulted particle dispersions of AEMP and AEPP in water to bagasse-based paper sheets provided excellent results. For strength properties, the results showed that, the extent of improving is not only dependent of fluorescent compound but depending also on average particle size. There was a good relation between the decreases of particle size, under the effect of sonication, with the improvement in quality number (Q_z). Moreover treating with morphology group-containing fluorescence compound (AEMP) achieved relatively high improvement in double fold property of paper sheets, compared with (AEPP).

It is surprising to notice that these investigated compounds, beside they provided thermal stability to treated paper sheets, also retarded the degradation, and decreased the formation of levoglucosan, and consequently the weight loss. The weight loss of volatilization stage is about 75 - 70.5%, and the final degradation stages are about 95.2 - 90 %. This means that, the fluorescence heterocyclic compounds, in addition to provide thermal stability to paper sheets, also exhibit, to some extent, fire resistance property to the produced treated paper.

The unfalsifiable safety property of the treated documents by erasures technique showed that, fluorescent compounds, especially with lower particle size, are penetrated inside paper sheets which makes it difficult against falsify.

Acknowledgment

This research work was supported through the Executive Program of Scientific and Technological Cooperation between Egyptian Ministry for Scientific Research and Italian Ministry of Foreign Affairs.

5. References

1. ANSI/NISO Z39.48-1992. Permanence of Paper for Publications and Documents in Libraries and Archives Published by NISO Press United States of America, R2002.
2. Basta AH. The Role of Chitosan in Improving the Ageing Resistance of Rosin-alum Sized Paper Sheets. Resturator 2003, 24: 106-117.
3. Basta AH. Performance of Improved Polyvinyl Alcohol as Ageing Resistance Agent of Rosin Sized Paper and in Restoration Purpose**.** Resturator 2004, 25: 129-140.
4. Basta AH, El-Saied H. New approach for utilization of cellulose derivatives metal complexes in preparation of durable and permanent colored papers. Carbohydrate Polymers 2008, 74: 301-308.
5. Lojewski T, Miskowiec P Missori, M.; Lubanska, A.;Proniewicz, L.M. and Lojewska, J. (2010). FTIR and UV/vis as methods for evaluation of oxidative degradation of model paper: DFT approach for carbonyl vibrations, Carbohydrate Polymers 2010;. 82: 370–375.
6. Malesic, J., Kolar, J.;. Strlic, M...Effect of pH and carbonyls on the degradation of alkaline paper: factors affecting ageing of alkaline paper', Restaurator 2002, 23: 145-153.
7. Basta, A.H, El-Saied, H.. Performance of improved bacterial cellulose application in the production of functional paper; Journal of Applied Microbiology 2009, 107 (6): 2098-2107.
8. Mosca Conte A, Pulci O, Knapik A, Bagniuk J, Del Sole R, Lojewska J, Missori, M. Role of Cellulose Oxidation in the Yellowing of Ancient Paper. Physical Review 2012,108: 158301-158301-5.
9. Corsaro C, Mallamace D. Lojewska J, Mallamace F, Pietronero L, Missori M. Molecular degradation of ancient documents revealed by 1H HR-MAS NMR spectroscopy. Scientific Reports 2013**,** 3: 2896-1-2896-10.
10. Brunelle RL, Reed RW. Forensic Examination of ink and paper, Charles. Thomas, Springfreld, IL., 1984.
11. Honnorat A, Raux L, Riou C.. Unfalsifiable safety paper, US patent no 4,725,497, 1988.

12. Basta AH, Girgis AS, El-Saied H. Fluorescence behavior of new 3-pyridinecarbonitrile containing compounds and their application in security paper. Dyes and Pigments 2002, 54: 1-10.

13. Mishriky N, Asaad F M, Girgis AS, Ibrahim YA.. New pyridine carbonitriles from fluoro arylpropenones. Recueil des Travaux Chimiques des *Pays-Bas* 1994, 113**: 35-39.**

14. Basta AH, Girgis AS, El-Saied H, Mohamed MA. Synthesis of fluorescence active pyridinedicarbonitriles and studying their application in functional paper. Materials Letters 2011, 65: 1713–1718.

15. Fu H-B and Yao J-N (2001) Size Effects on the Optical Properties of Organic Nanoparticles. Journal of the American Chemical Society 123:1434-1439

16. Xiao D, Xi L, Yang W, Fu H, Shuai Z, Fang Y and Yao J (2003) Size-Tunable Emission from 1,3-Diphenyl-5-(2-anthryl)-2-pyrazoline Nanoparticles. Journal of the American Chemical Society 125:6740-6745

17. Kim H Y, Bjorklund T G, Lim S-H and Bardeen C J (2003) Spectroscopic and Photocatalytic Properties of Organic Tetracene Nanoparticles in Aqueous Solution. Langmuir 19:3941-3946

18. Abyan M, Bîrla L, Bertorelle F and Fery-Forgues S (2005) Morphology control of organic luminescent microcrystals and approach of their optical properties. Comptes Rendus Chimie Matériaux moléculaires 8:1276-1281.

19. Fery-Forgues S, Abyan M and Lamere J-F (2008) Nano- and Microparticles of Organic Fluorescent Dyes. Annals of the New York Academy of Sciences 1130:272-279

20. Destrée C, George S, Champagne B, Guillaume M, Ghijsen J and Nagy J B (2008) J-complexes of retinol formed within the nanoparticles prepared from microemulsions. Colloid and Polymer Science; 286:15-30.

21. Fang Q, Wang F, Zhao H, Liu X, Tu R, Wang D and Zhang Z. Strongly Coupled Excitonic States in H-Aggregated Single Crystalline Nanoparticles of 2,5-Bis(4-methoxybenzylidene) Cyclopentanone. The Journal of Physical Chemistry B 2008; 112:2837-2841

22. Al-Kaysi R O, Mueller A M, Ahn T-S, Lee S and Bardeen C J Effects of Sonication on the Size and Crystallinity of Stable Zwitterionic Organic Nanoparticles Formed by Reprecipitation in Water. Langmuir 2005; 21:7990-7994.

23. Kasai H, Nalwa S H, Oikawa H, Okada S, Matsuda H, Minami N, Kakuta A, Ono K, Mukoh A and Nakanishi H. A Novel Preparation Method of Organic Microcrystals. Jpn. Journal of Applied Physics 1992; 31:L1132-L1134

24. Kasai H, Kamatani H, Okada S, Oikawa H, Matsuda H and Nakanishi H. Size-Dependent Colors and Luminescences of Organic Microcrystals. Jpn. Journal of Applied Physics 1996; 35:L221-L223
25. Kang P, Chen C, Hao L, Zhu C, Hu Y and Chen Z. A novel sonication route to prepare anthracene nanoparticles. Materials Research Bulletin 2004; 39:545-551
26. Perepogu A and Bangal P. Preparation and characterization of free-standing pure porphyrin nanoparticles. Journal of Chemical Sciences 2008; 120:485-491
27. Missori,M.; De Spirito, M.; Ferrari, L.; Selci, S.; Gnoli, A.; Arcovito, G.; Girgis, A.S.; El-Saied, H.and Basta, A.H. Preparation and optical properties of 2-Amino-6-ethoxy-4-[4-(4-morpholinyl)phenyl]-3,5pyridinedicarbonitrile nanoparticles: a security marker for paper documents, Pt. I. Journal of Nanoparticle Research 2012; 14: 649-1-12.
28. McNamara W B, Didenko Y T and Suslick K S. Sonoluminescence temperatures during multi-bubble cavitation. Nature 1999; 401:772-775.
29. Suslick K S (1990) Sonochemistry. Science 247:1439-1445
30. Teo B M, Grieser F and Ashokkumar M. High Intensity Ultrasound Initiated Polymerization of Butyl Methacrylate in Mini-and Microemulsions. Macromolecules 2009; 42:4479-4483.
31. Bertorelle, F., Lavabre D, and Fery-Forgues S., Dendrimer-Tuned Formation of Luminescent Organic Microcrystals. Journal of the American Chemical Society, 2003. 125(20): 6244-6253.
32. Andreasi Bassi F, Arcovito G, De Spirito M, Mordente A, Martorana G E. Self-similarity properties of alpha-crystallin supramolecular aggregates. Biophysical Journal 1995; 69: 2720-2727
33. De Spirito M, Arcovito G, Papi M, Rocco M, Ferri F. Small-and wide-angle elastic light scattering study of fibrin structure. Journal of Applied Crystallography 2003; 36:636-641
34. Maulucci G, De Spirito M, Arcovito G, Boffi F, Castellano A C, Briganti G. Particle size distribution in DMPC vesicles solutions undergoing different sonication times. Biophysical Journal 2005; 88:3545-3550
35. Provencher S. CONTIN: a general purpose constrained regularization program for inverting noisy linear algebraic and integral equations. Computer Physics Communications 1982; 27:229-242
36. Mazzuca C, Orioni B, Coletta M, Formaggio F, Toniolo C, Maulucci G, M De Spirito, Pispisa B, Venanzi M, Stella L.. Fluctuations and the rate-limiting step of peptide-induced membrane leakage. Biophysical Journal 2010. 99:1791-1800.
37. International Standard, ISO 187, 1990 (E).

38. The institution of paper chemistry, Appleton, Wisconsin (1952)., institute method no. 411-5 Oct. 1st (1951).

39. Levdik, I; Inshakov, M.D.; Misyurova, E.P.; Nikitin, V.N. Study of pulp structure by infra-red spectroscopy.*Tr. Vses Nauch. Issled. Irst. Tsellyul Bum. Prom*.1967, *52*: 109..

40. Coats, A.W; Redfern, J.P.Kinetic parameters from thermogravimetric data. *Nature.* 1964, *201*, 68.

41. Basta AH. Preparation, characterization and properties of paper sheets made from chemically modified wood pulp treated with metal salts International Journal of Polymeric Materials 1998, 42:1-26.

42. Hong Q L, Hardcastle J, McKeown R A J, Marken F and Compton R G (1999) The 20 kHz sonochemical degradation of trace cyanide and dye stuffs in aqueous media. New J. Chem. 23:845-849

43. Serebrenikov P. Chemical Methods of Fire. Zbornik Trud, CNILCHI 1934; 2, 407-9 .

44. Shafizadeh F, Lai YZ, Mclinlyre CR.. Thermal degradation of 6-chlorocellulose and cellulose-zinc chloride mixture. Journal Applied Polymer. Science. 1978., 22, 1183 - 1193.

45. Shafizadheh F, Furneauk RM, Cochern TG, School JP, Sakai YS.. Production of levoglucosan and glucose from pyrolysis of cellulosic materials. Journal Applied Polymer. Science 1979, 23, 3525- 3539.

Table 1: Conditions of preparation of fluorescence particles and their properties.

Sample code	Fluorescence Cpd.	Solution Volume	Water volume	Sonication Power (W)	Process time (min)	Temperature (^{o} C)	$\langle R_h \rangle \pm \sigma$ (nm)	$\sigma/\langle R_h \rangle$	zeta potential
S1 AEMP	3c	100 ul	10 ml	12.5	1	0	479±378	0.79	
S2 AEMP	3c	100 ul	10 ml	12.5	5	0	264 ±137	0.52	approx -20 mV
S3 AEMP	3c	100 ul	10 ml	12.5	30	0	97±39	0.40	
S4 AEPP	3d	100 ul	10 ml	12.5	1	0	499 ± 265	0.53	
S5 AEPP	3d	100 ul	10 ml	12.5	5	0	224± 110	0.49	approx -10 mV
S6 AEPP	3d	100 ul	10 ml	12.5	30	0	240±139	0.58	

Process conditions used to obtain the AEMP and AEPP particles with the indication of the size and size distribution observed ($\langle R_h \rangle$*is the mean hydrodynamic radius,* $\sigma/\langle R_h \rangle$ is the polydispersity index of the size distribution; zeta potential is the electric potential between nanoparticles which is correlated to the stability of the nanoparticles suspension

Table 2 Main IR-absorption bands and measurements of untreated and fluorescence nano-particles treated paper sheets.

Paper Sample	MHBS	ν_{OH} or ν_{NH} (stretching)		ν_{CH} (stretching)		$\nu_{C=O}$ (stretching) Amide I & II(1558–1705cm^{-1})		ν_{OH} or ν_{NH} (bending)		ν_{C-O} 1000–1280 cm^{-1}		ν_{CH} (rocking)	
		cm^{-1}	E/A1050	cm^{-1}	E	cm^{-1}	E	cm^{-1}	E	cm^{-1}	E	cm^{-1}	E
Untreated	0.917	3856.35	0.294	2933	0.522	1730.2	0.231	1466.9	0.293	1279	0.184	927.0	0.275
		3752.22	0.295	2857	0.465	1679.1	0.259	1375.3	0.203	1158.4	0.263	879.8	0.992
		3335.67	0.479			1533.5	0.2461	1322.4	0.171	1033.1	1.00	741.9	0.157
S1 AEMP	0.887	3745.5	0.259	2930	0.448	1725.4	0.235	1468.9	0.326	1270.3	0.189	887.5	0.348
		3659.7	0.283	2860	0.395	1646.3	0.319	1329.1	0.209	1109.3	1.122	841.2	0.159
		3322.2	0.398			1560.5	0.307			1111.2	0.543	645.5	0.474
		3177.5	0.352							1031.2	1.00	594.4	1.183
S2 AEMP	0.934	3679.9 (sh)	0.252	2925	0.433	1720.6(s)	0.200	1464.1	0.302	1279.9	0.245	899.1	0.367
			0.404	2865	0.364	1655.011	0.286	1431.3	0.294	1109.3 (sh)	0.568	779.5	0.276
		3328.9				1563.4(sh)	0.239	1370.6	0.265	1036	1.00	659.9	0.630
S3 AEMP	0.9529	3755.1	0.153	2931	0.394	1719.6	0.149	1464.1	0.229	1276.1	0.127	887.5	0.189
		3289.4	0.376	2860	0.326	1653.1	0.222	1435.1	0.210	1150.7	0.204	781.4	0.142
						1552.8	0.173	1371.5	0.155	1108.3	0.511	649.3	0.526
								1322.4	0.134	1032.1	1.00		
S4 AEPP	0.9674	3743.5 (sh)	0.394	2931	0.573	1711.9(s)	0.423	1466.9	0.475	1263.5	0.419	893.3	0.502
			0.481	2860	0.526	1658.9	0.46	1342.6	0.440	1161.3	0.474	841.2	0.382
		3613.4	0.554			1540.3(sh)	0.449			1111.2	0.685	755.4	0.497
		3299.9								1032.1	1.00	650.3	0.754
S5 AEPP	0.989	3753.2 (sh)	0.1200	2929	0.440	1718.7	0.129	1461.2	0.221	1276.1	0.158	900.0	0.223
			0.435	2867	0.345	1653.1	0.207	1435.2	0.222	1159.41105	0.243	792.9	0.083
		3335.7						1368.6	0.200	1032.1	0.543	642.5	0.178
								1322.3	0.188		1.0		0.189
S6 AEPP	1.225	3751.3	0.140	2860	0.368	1718.7s	0.133	1461.2	0.223	1289.6	0.124	887.5	0.219
		3335.7	0.429			1663.7	0.189	1368.6	0.182	1163.3	0.216	841.2	0.068
		(sh)	0.451							1104.4	0.550	645.5	0.450
		3229.7								1034.0	1..0	594.4	

Where, MHBS : $A_{OH(Str.)}$ /$A_{CH\ (Str.)}$

Table 3: Kinetic parameters of un- and fluorescence treated bagasse-based paper sheets.

Paper sample	stage	Temp. range °C	DTG peak temp. °C	"n"	-r	Se	E_a kJ/ mole	Wt. (final)
Untreated	1st	50- 102.41	-	-	-	-	-	94.563
	2nd	209.19-343.11	289.49	1.5	0.989	0.17	131	23.485
	3rd	380.6 - 469.96	438.8					3.16
S1 AEMP	1st	50- 125.09	-	-	-	-	-	93.555
	2nd	223.39- 345.96	307.68	1.5	0.986	0.14	143.32	29.498
	3rd	381.87 – 477.01	424.46					9.797
S2 AEMP	1st	50- 99.44		-	-	-	-	93.374
	2nd	226.33 -344.4	302.2	1.5	0.991	0.15	138.38	25.403
	3rd	392.03 -487.14	452.51					5.833
S3 AEMP	1st	50- 109.37		-	-	-	-	93.355
	2nd	233.46-356.07	305.68	1.5	0.984	0.19	162.07	23.94
	3rd	392.1 -491.41	455.6					6.351
S4 AEPP	1st	50-137.24		-	-	-	-	91.686
	2nd	210.1- 346.22	303.81	1.5	0.946	0.22	131.15	24.984
	3rd	389.1-478.5	455.26					6.781
S5 AEPP	1st	50- 102.29		-	-	-	-	92.866
	2nd	232.04- 344.8	296.52	1.5	0.983	0.19	148.08	27.945
	3rd	392.87- 516.04	459.85					7.846
S6 AEPP	1st	50- 115.37		-	-	-	-	91.846
	2nd	240.78 -360.49	304.84	1.5	0.989	0.16	152.13	22.02
	3rd	386.3 -498.7	452.6					4.751

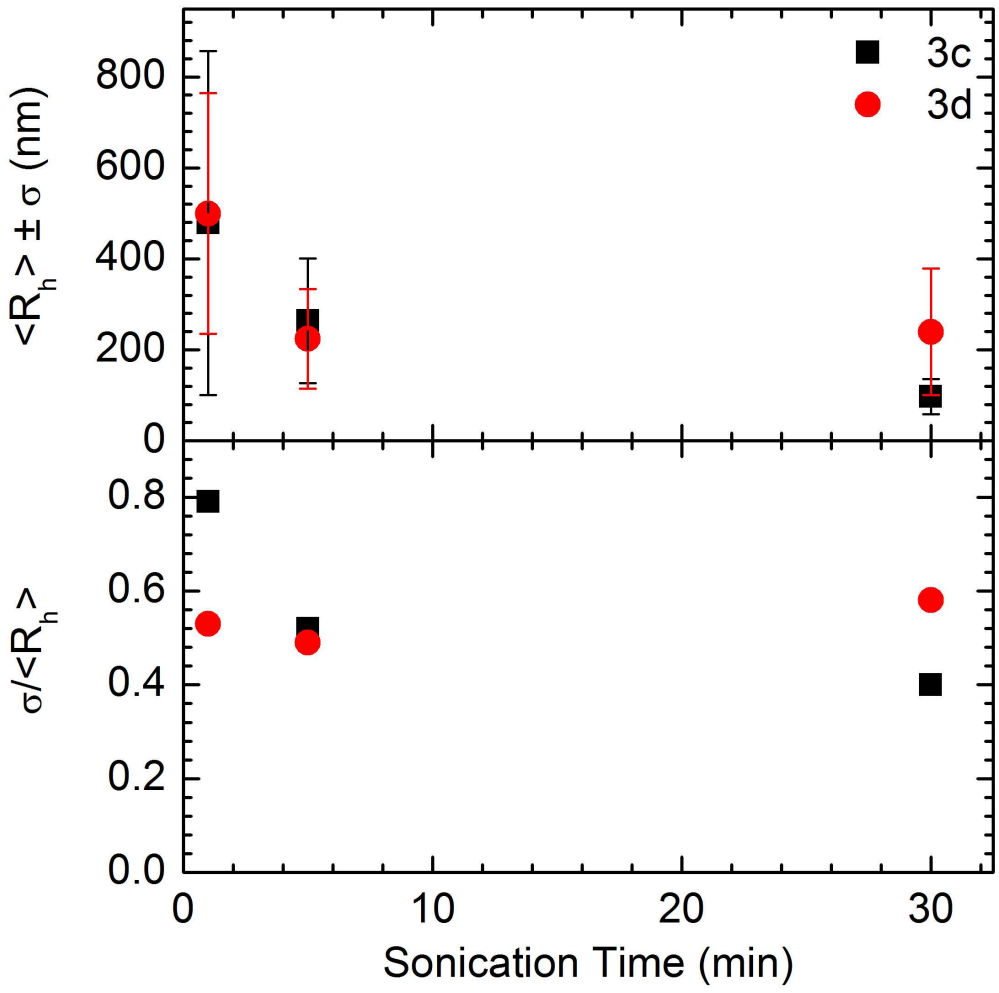

Figure 1. The mean hydrodynamic radii ‹R_h› together with the polydispersity index of the size distribution (σ/‹R_h›) of the **3c** (AEMP) and **3d** (AEPP) particles dispersed in water.

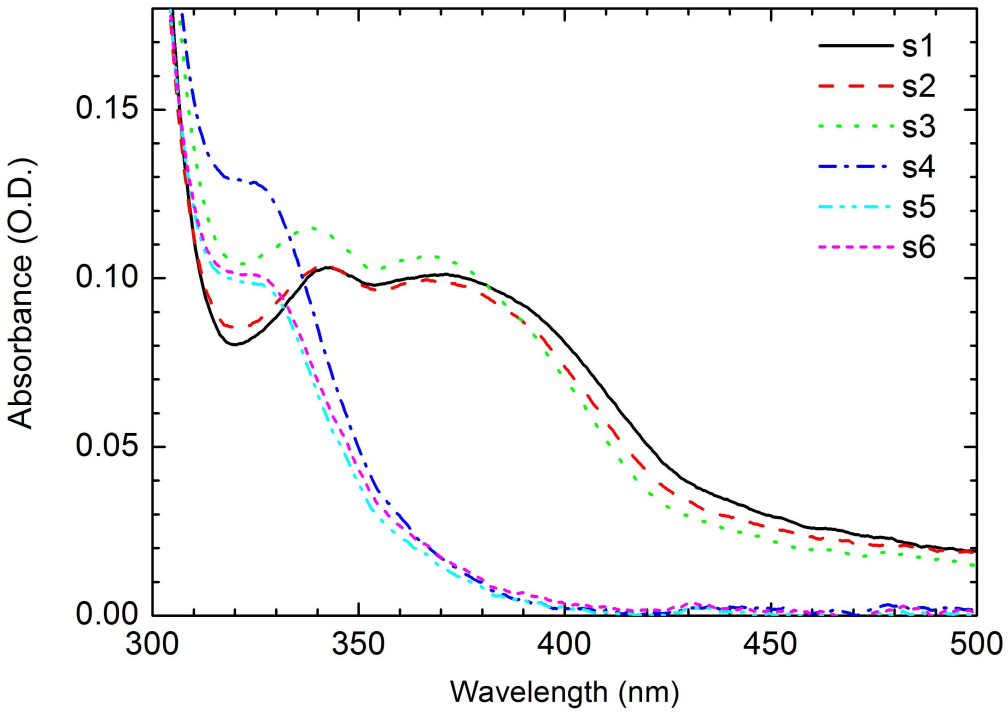

Figure 2-a Ultraviolet-visible absorption spectrum of fluorescence heterocyclic sonicated AEMP and AEPP particles in water suspension.

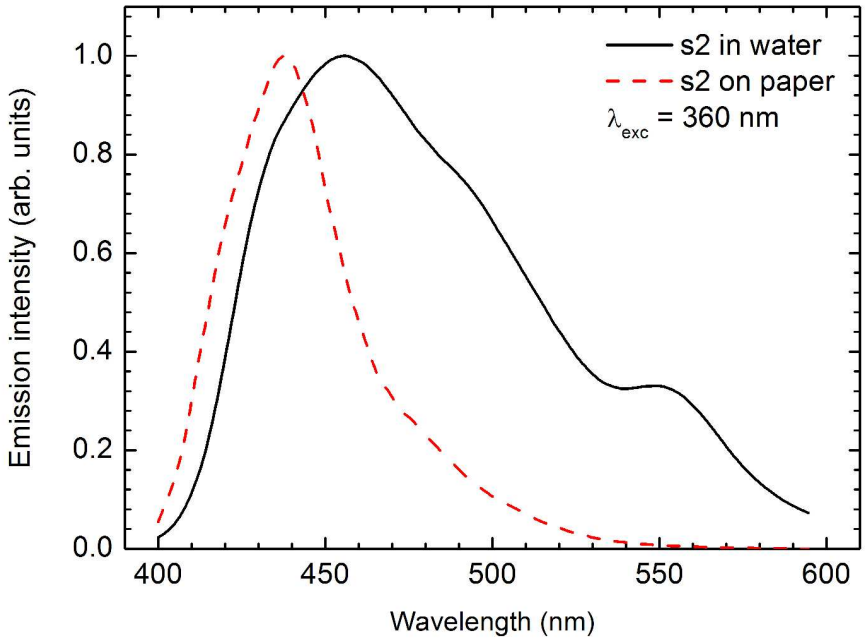

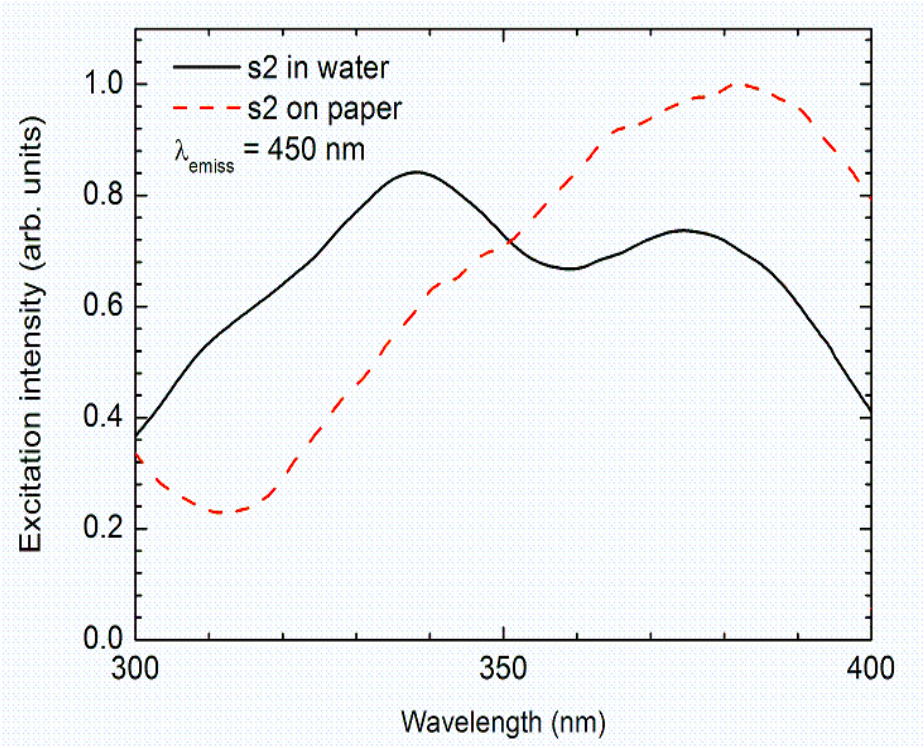

Figure 2-b. Excitation and emission bands of AEMP particles in water and on paper substrate.

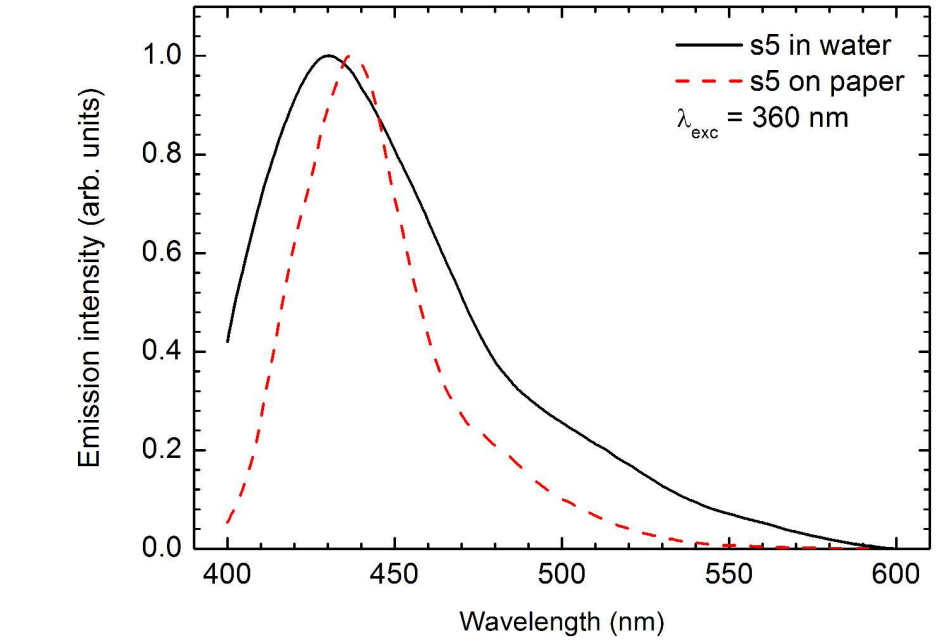

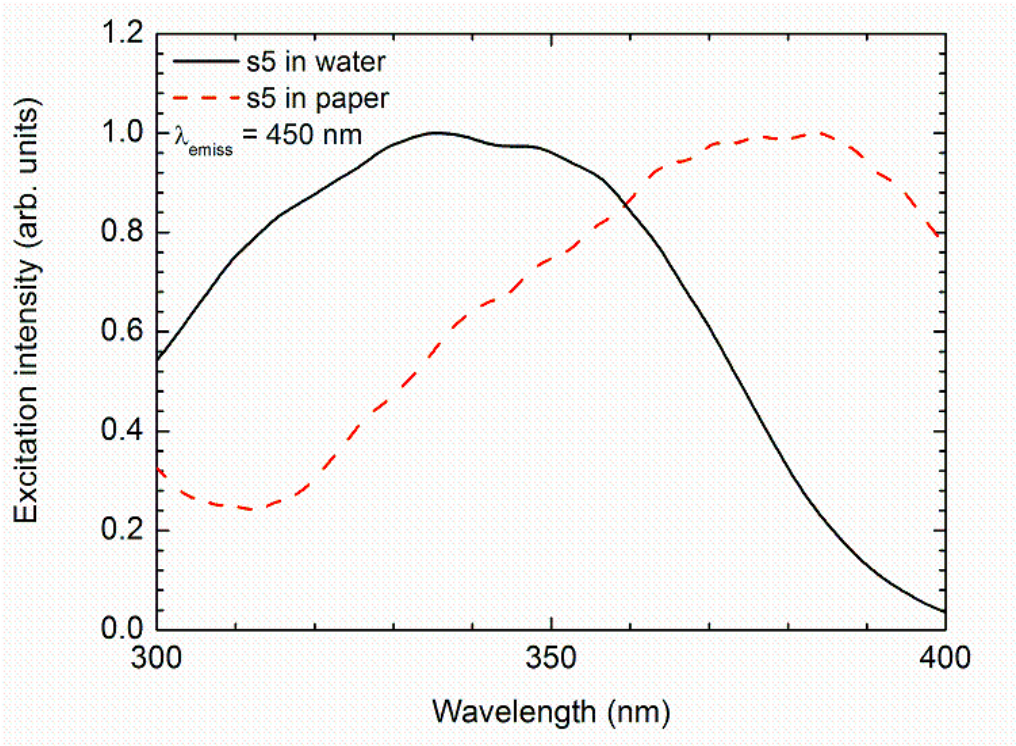

Figure 2-c Excitation and emission bands of AEPP particles in water and on paper substrate.

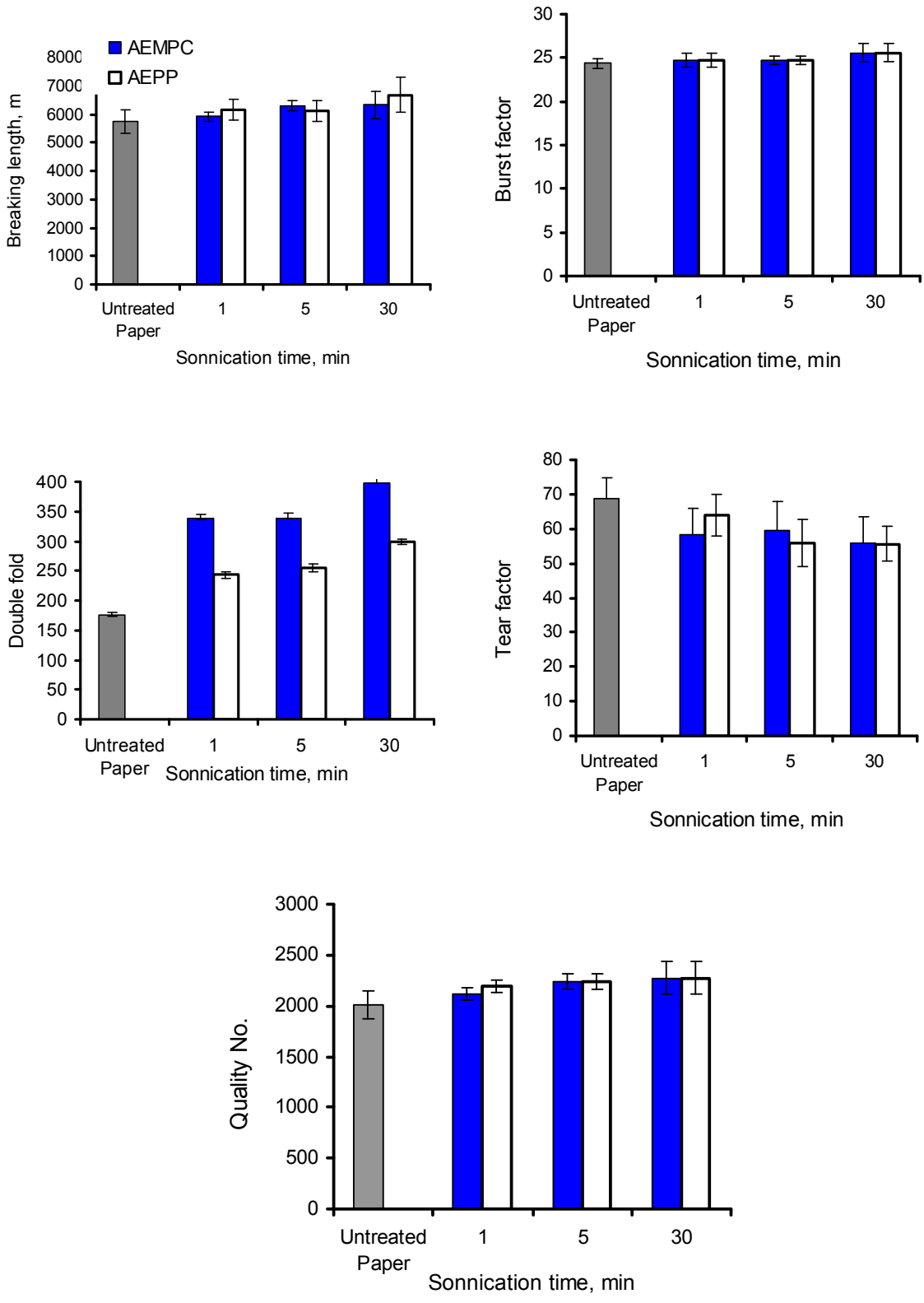

Figure 3. Strength properties of surface treated paper sheets with sonicated morpholinyl containing fluorescence (AEMP) and piperidinyl containing fluorescence (AEPP) compounds

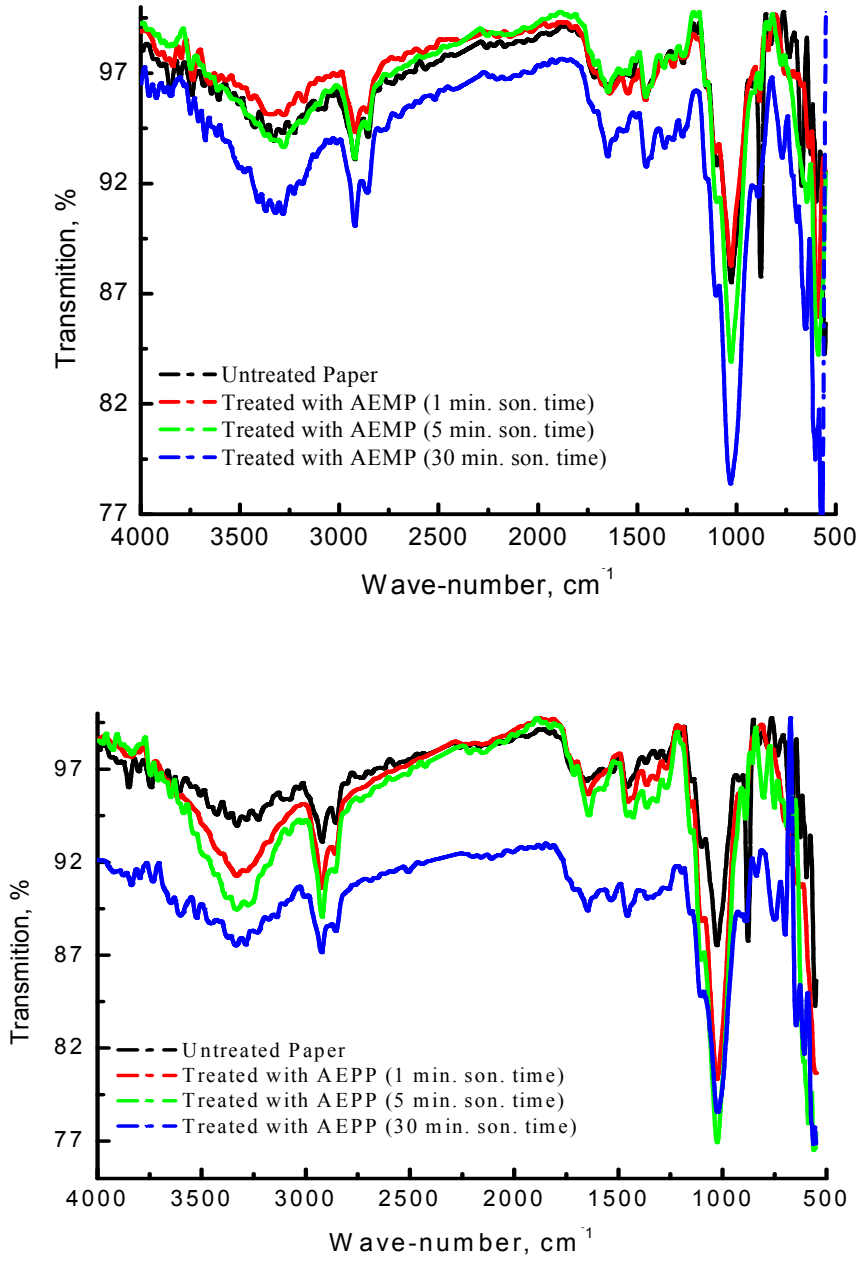

Figure 4. FT-IR spectra of surface treated paper sheets with sonicated morpholinyl containing fluorescence (AEMP) and piperidinyl containing fluorescence (AEPP) compounds

Untreated

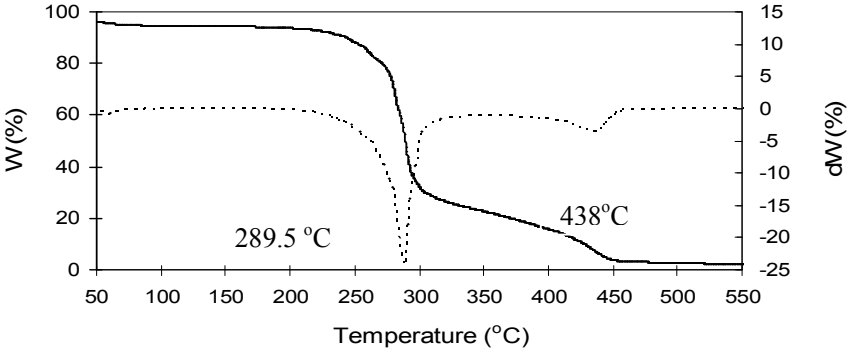

AEMP-S1

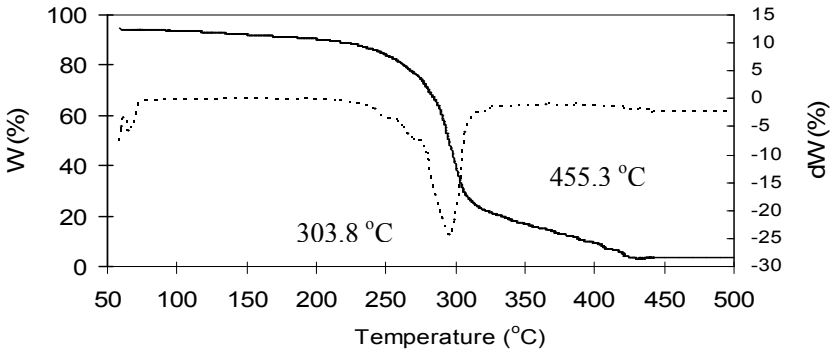

AEMP-S2

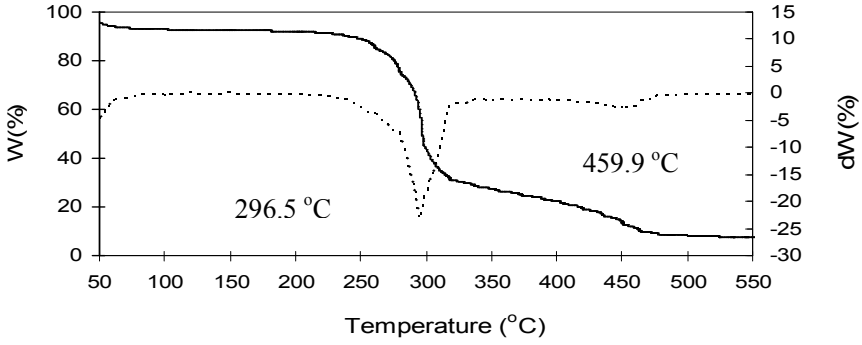

AEMP-S3

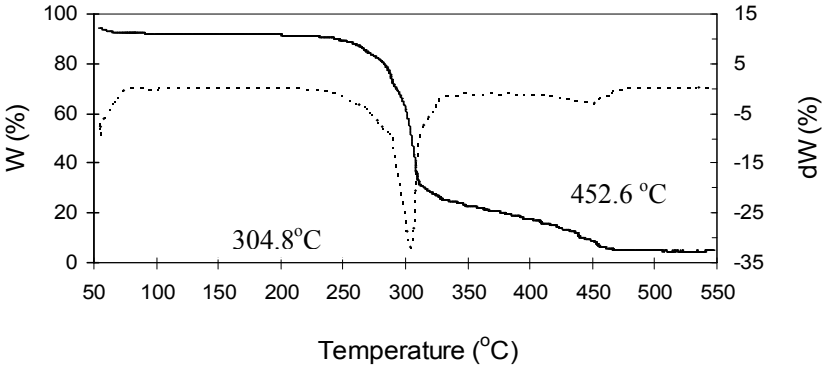

36

Fig.ure 5-a TGA and DTGA curves of surface treated paper sheets with sonicated morpholinyl containing fluorescence (AEMP)

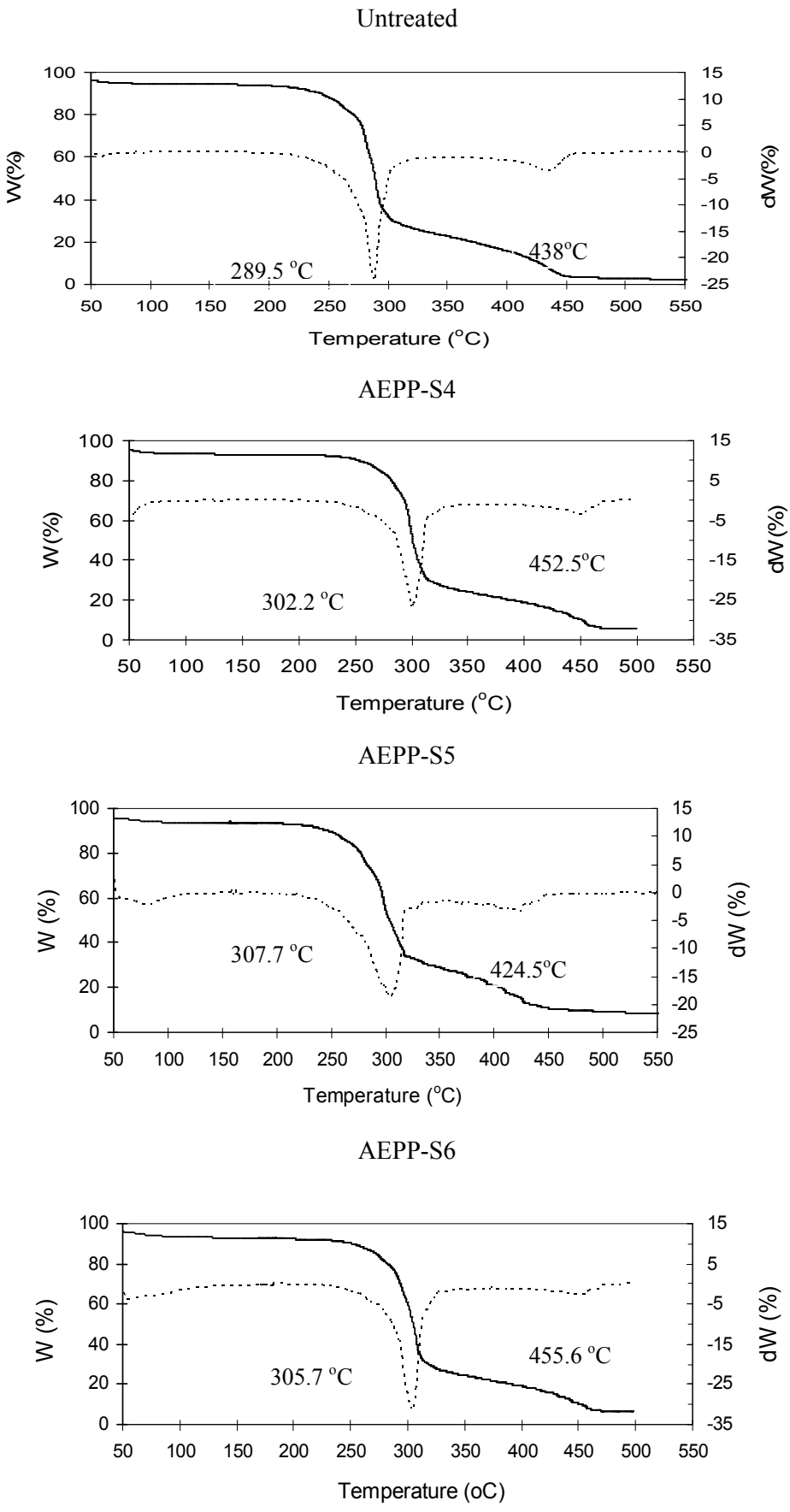

37

Figure 5-b.: TGA and DTGA curves of surface treated paper sheets with sonicated piperidinyl containing fluorescence (AEPP)

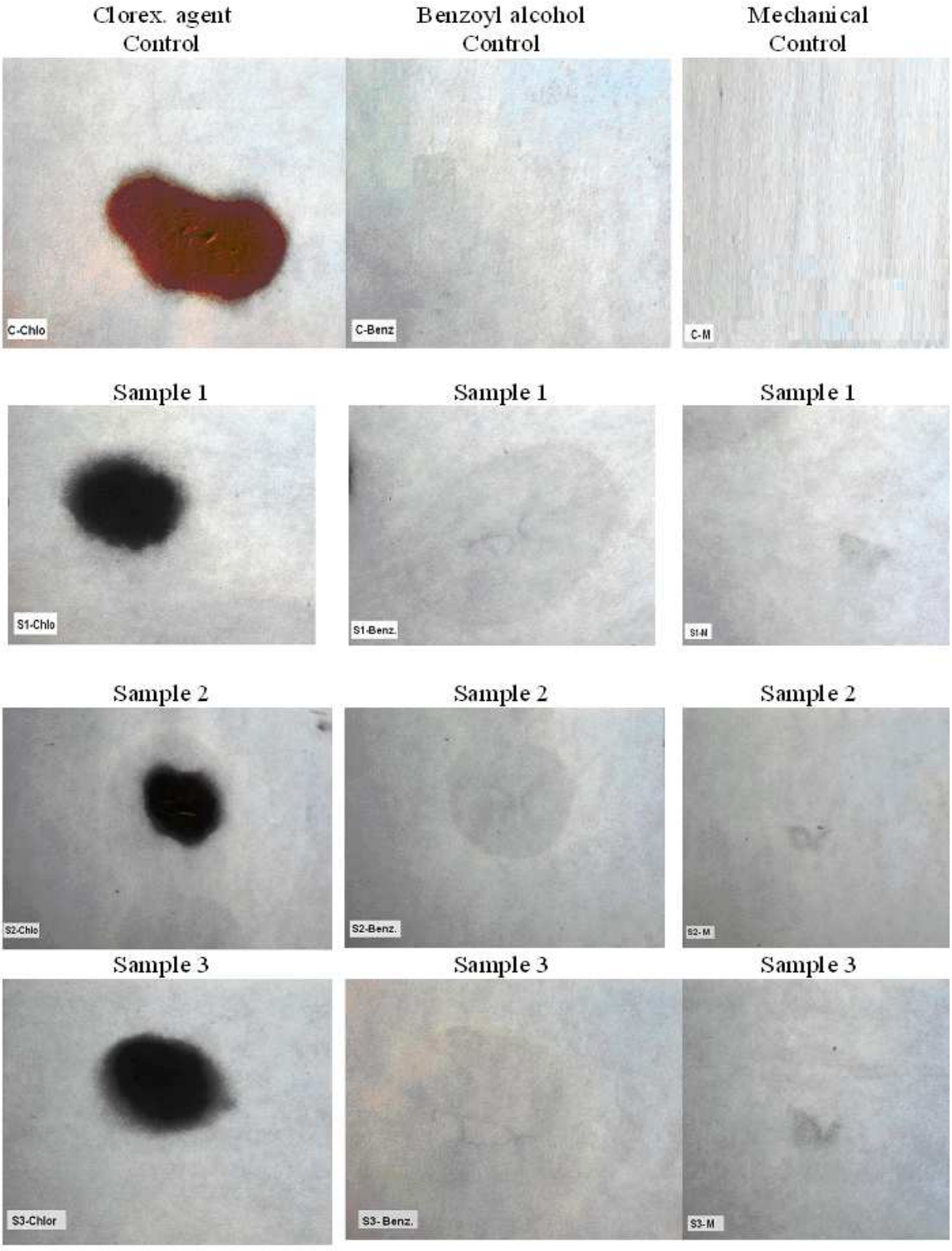

Figure 6-a. Chemical and mechanical erasure of surface treated paper sheets with morpholinyl-containing fluorescence compound (AEMP)

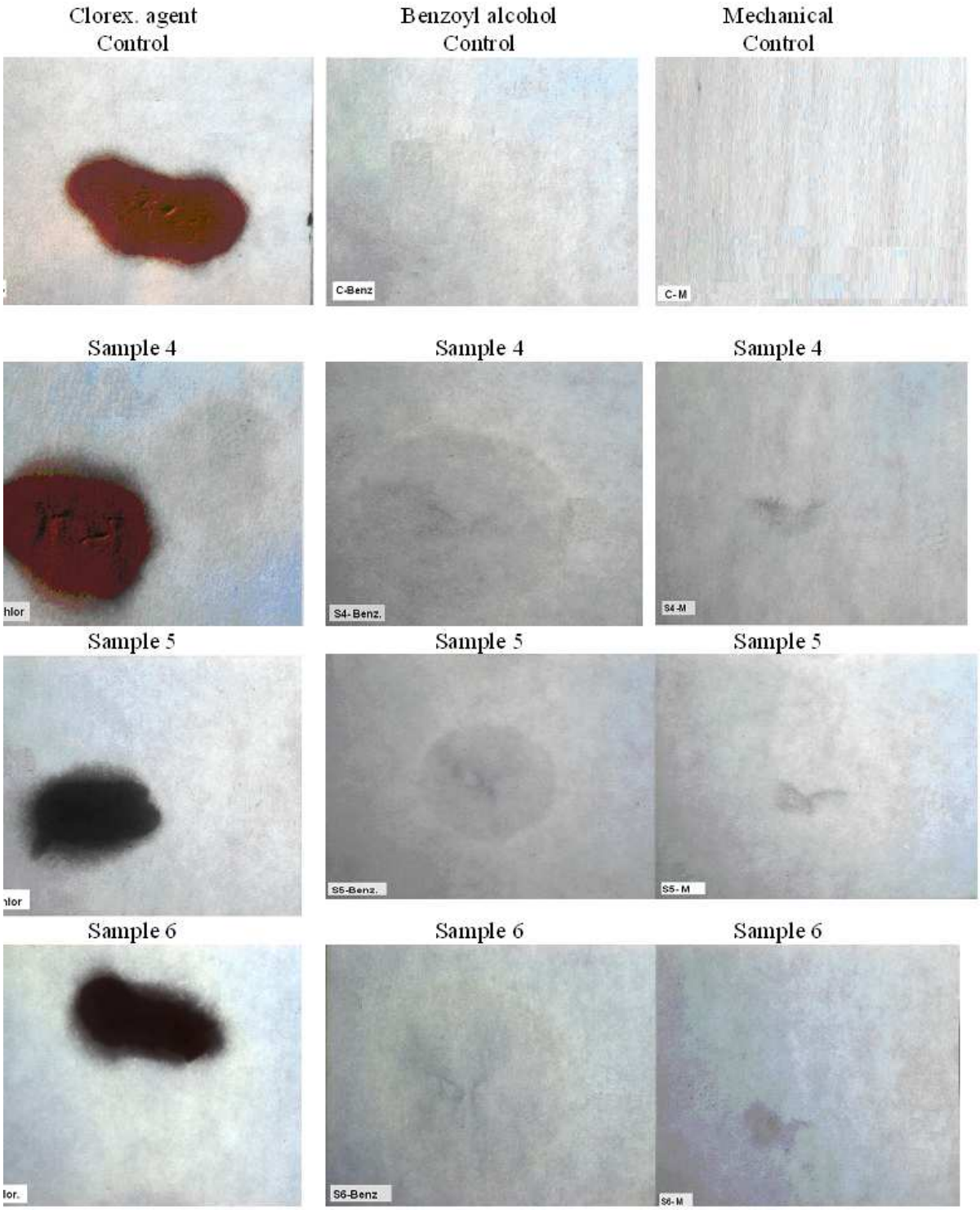

Figure 6-b. Chemical and mechanical erasure of surface treated paper sheets with Piperidinyl-containing fluorescence compound (AEPP)